Tracking of Neoclassical Tearing Modes in TCV using the Electron Cyclotron Emission diagnostics in quasi-in-line configuration

N. Rispoli[a,*], C. Sozzi[a], L. Figini[a], D. Micheletti[a], C. Galperti[b], M. Fontana[b], E. Alessi[a], S. Coda[b], S. Garavaglia[a], T. Goodman[b], M. Kong[b], M. Maraschek[c], A. Moro[a], L. Porte[b], O. Sauter[b], U. Sheikh[b], D. Testa[b], EUROfusion MST1 Team[1], and TCV team[2]

[a] *Istituto di Fisica del Plasma "Piero Caldirola" - CNR, Milano, Italy*
[b] *Ecole Polytechnique Fdrale de Lausanne (EPFL), Swiss Plasma Center (SPC), Lausanne, Switzerland*
[c] *Max Planck Institute for Plasma Physics, Garching, Germany*

Abstract

An important goal of the control system in a tokamak is the suppression of magneto-hydrodynamic (MHD) instabilities with low m, n (poloidal and toroidal mode numbers), which can influence the confinement time of energy and particles and possibly lead to plasma disruption. These instabilities, which appear as rotating magnetic islands, can be reduced or completely suppressed by a current driven by electron cyclotron waves (ECW) accurately located within the island. A fundamental requisite for this control technique is the ability to identify the island parameters (amplitude and radial position) and to vary accordingly the ECW deposition location. Here we describe a control scheme of the steering mirror of the ECW source based on the real-time tracking of the island radial position realized using only the electron cyclotron emission (ECE) diagnostics in quasi-in-line configuration, i.e. with toroidal anti-parallel propagation of the ECW and ECE beams. The successful experimental proof of principle of this scheme, tested on the TCV tokamak, is here reported.

Keywords:
TCV
Neoclassical Tearing Mode
Real Time Control
Tokamak

1. Introduction

One of the limiting factors of the tokamak performance arises from the magnetic-hydrodynamic instabilities. They present themselves as rotating islands, corresponding to a flat region in electron temperature profile, that reduce the plasma confinement and, depending on their size and growth rate, can lead to disruptions. The reduction or suppression of magneto-hydrodynamic instabilities, in particular of Neoclassical Tearing Modes (NTMs), can be performed through localized current driven by Electron Cyclotron Wave (ECW)([1]). This is a challenging control task that requires: the detection of magnetic island spatial position; steering of the mirror in the correct position and the triggering of the electron cyclotron ECW sources. To achieve this goal a few computational steps are needed, such as magnetic equilibrium reconstruction, ECW beam tracing, correct time phasing and angular steering of the ECW injection. To successfully apply EC waves for NTM control it is important that the island is detected as early as possible and that its localization is identified with an equal or better accuracy than the radial extension of the ECW beam width.

A closed loop control scheme using quasi-in-line configuration, with toroidal anti-parallel propagation of the ECW and ECE beams, allows real time tracking and NTMs suppression without the need of knowing *a priori* the exact mirror steering angle, without precise magnetic equilibrium reconstruction and without beam tracing computation. The proof of principle of this control scheme was demonstrated on TCV, using different values of poloidal and toroidal shift between ECW and ECE, and is described in this paper. The toroidal injection angle is kept constant and equal for both ECE and ECW, while the poloidal aiming of the ECW antenna keeps into account the poloidal shift.

A brief description of TCV control system and NTM control scheme are presented in section 2. The detection algorithm (DA) is described in section 3. The main results are reported in section 4.

*Corresponding author
Email address: natale.rispoli@ifp.cnr.it (N. Rispoli)
[1] See the author list of H. Meyer et al 2017 Nucl. Fusion 57 102014
[2] See the author list of S. Coda et al 2017 Nucl. Fusion 57 102011

2. TCV System and NTM Control scheme

TCV is a medium sized tokamak with major radius of $0.88m$, minor radius of $0.25m$ and maximum toroidal field of $1.5T$ ([2]). A distributed digital RT control system, with highly modular structure, and connected with a wide range of plasma diagnostics permit to develop control algorithms independently and to be integrated into the multi-controller environment.

The control schemes, realized in such environment, have been tested using ECE radiometer ([3]) with $L3$ launcher transmission line and ECW with launcher $L1$ or $L2$, see Figure 1. $L1$ and $L3$ are at same toroidal location with a poloidal shift, while $L2$ is at same poloidal shift but in a different toroidal sector. All launchers ($L1$, $L2$ and $L3$) are identical antenna systems based on steerable mirrors. Figure 1 shows the experimental configuration (left) and the simplified control scheme (right).

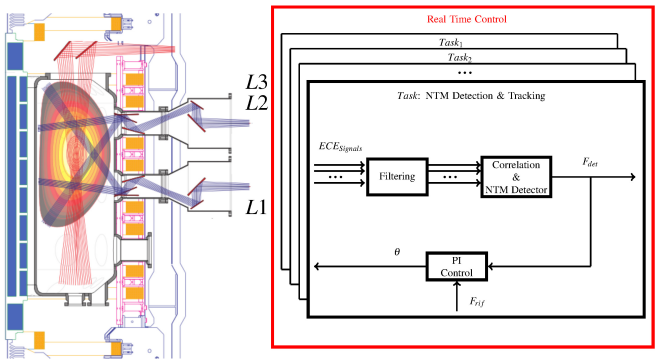

Figure 1: Simplified scheme of NTM detection and mirror control

The ECE system has 24 channels, divided in: 1) 12 channels on low field side (LFS) $66.15 \leq f \leq 82.15\ GHz$; 2) 12 channel on high field side (HFS) $85.48 \leq f \leq 101.48\ GHz$. Signals, collected through this system, are used to detect the plasma frequency location of NTM instability.

The detected frequency (F_{isl}) is used by the control to move $L3$ mirror at angle corresponding to target frequency (F_{rif}), which is the angle where the frequency detected by ECE radiometer is equal to ECW frequency ($82.7GHz$). The mirror on $L1$ or $L2$ was moved accordingly to $L3$ and the ECW power is activated when the target frequency is reached.

The control has been realized using only a proportional-integral-derivative (PID) action for feedback and without a feedforward action. The PID parameters have been chosen with trial and error method during the preliminary setup phase. No derivative (D) action has been used in the control loop to avoid abrupt changes in the reference signal sent to the actuator when the instability appear and the detection starts.

3. Detection Algorithms

The algorithm by Berrino et al. ([4]), that uses only ECE signals, has been used to detect the island location in the frequency space. Correlating adjacent frequency channels signals, the algorithm detects the phase opposition between ECE signals on opposite sides of frequency corresponding to the rational flux surface. It can be divided into three different calculation steps.

Defined $ECE_i(k)$ the signal measured by the i-th ECE channel at frequency f_i and at time k, in the first step the oscillation information is extracted from signals using a band pass filter and the results (δECE_i) is divided by the root mean square value:

$$\overline{\delta ECE}_i(k) = \frac{\delta ECE_i(k)}{\sqrt{\frac{1}{N_{rms}} \sum_{j=0}^{N_{rms}} \delta ECE_i(k-j)}} \qquad (1)$$

The correlation between adjacent ECE channels is calculated in the second step as:

$$C_i = \frac{1}{N_c} \sum_{j=0}^{N_c} \overline{\delta ECE}_i(k-j) * \overline{\delta ECE}_{i+1}(k-j) \qquad (2)$$

thus obtaining a set of N_{ECE} correlation functions C_i, N_{ECE} being the number of channels of the diagnostics.

In the third and final step, the effort is in identify the presence and location of the island ($\overline{f}_{isl}$). The island presence can be identified when the second derivative of correlation functions (C_i) exceeds a fixed threshold (s). The fixed threshold s is used to avoid false detections due to the measurement noise.

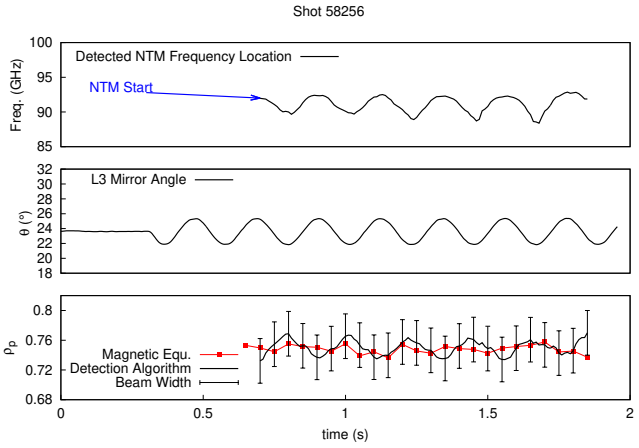

Figure 2: Frequency detected by DA algorithm (top), preprogrammed mirror steering (center) and minor radius of the emission region vs time (bottom)

A value $s = 0.06/\Delta f^2$, being $\Delta f = 1.46GHz$ the ECE channels spacing, does not produce false detections.This s value was found using a trial and error approach and experimental data of 3 shots with a preprogrammed mirror movement. Figure 2 shows the results of the setup procedure, with preprogrammed mirror movement and NTM at $q = 2$ rational surface, used to set the threshold level.

In Figure 2 (bottom) the comparison between the minor radius of the rational surface identified by the algorithm and the one reconstructed offline by the magnetic

equilibrium shows that the detected instability location is centered on the rational surface with an accuracy smaller than the ECE beam width. The oscillation seen by the DA is due to the mirror movement and to the island radial size extending across multiple ECE channels.

4. Results

The control scheme was tested on NTM instabilities on the rational surface $q = 2$. Due to technical problems in the operation and to the limited signal/noise of the LFS, only the HFS radiometer channels have been used. Under these conditions the minimum attainable frequency was 88 GHz, corresponding to 80.5 GHz on LFS. Therefore, since it is not possible to reach the ECW frequency, the triggering condition for the gyrotron can not bet realized unless the target frequency is changed to 88 GHz and an unavoidable error is accepted on firing position, corresponding to $\Delta\rho_p \simeq 0.02$. This was successfully done on Shot 58680.

Both $L1$ (Shot 58680, 59252) and $L2$ (Shot 59245) launchers have been used with similar results, only the results for the $L1$ launcher configuration are shown here.

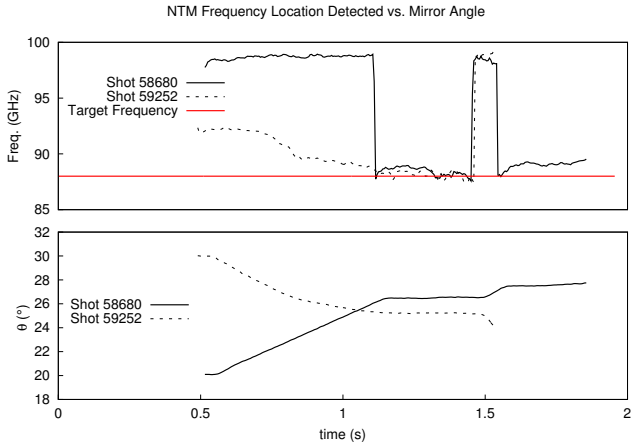

Figure 3: NTM frequency detection (top) and mirror steering (bottom) for TCV shot 58680 (solid line) and shot 59252 (dashed line).

Figure 3 (top) shows the frequency detection results and mirror steering (bottom) for two TCV shots, with mirrors starting position $\theta = 20^o$ (solid curve) and $\theta = 30^o$ (dashed line). The minor radius of the emission region as a function of the $L3$ angle and of the frequency, obtained in post-processing with the SPECE code([5]), is shown in figures 4 (shot 58680) and 5 (shot 59252). In these figures, dashed lines in the color code highlight the emission regions seen by the radiometer according to the angle of the mirror, continuous lines delimit the minimum and maximum angle spanned by the mirror during the experiment and the points indicate the position in which the DA identified the instability.

Experimental results show the DA capability to detect the NTM instability, with an error comparable with beam width, when $\theta > 25^o$. It is possible to notice the loss of

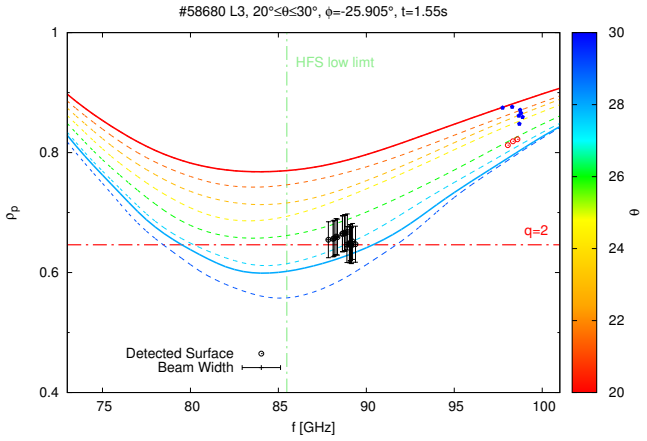

Figure 4: Minor radius of the emission region for Shot 58680 as function of $L3$ angle and frequency

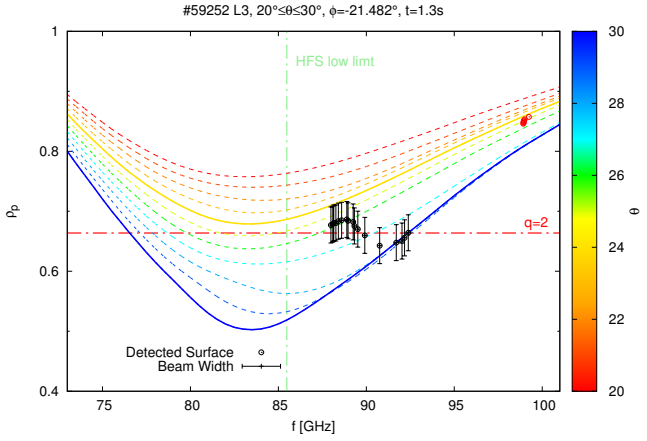

Figure 5: Minor radius of the emission region for Shot 59252 as function of $L3$ angle and frequency

precision in detection for $\theta < 25^o$ when there are no channels on opposite sides of instability (full points at the top right of the Figure 4). Under these conditions the algorithm detects the oscillations on the temperature signal and therefore the presence of an NTM instability, but it is not able to identify the exact spatial position. Moreover when the line of sight is tangent to the instability rational surface, at $25^o < \theta < 26^o$, a displacement of the plasma can lead to an error in the NTM spatial localization (empty points at the top right of the Figure 4 and 5). Similar conditions have already been discussed in [6] for the study of quasi-in-line configurations in ITER. These limitations can be solved or reduced by new DA exploiting the signals of all the ECE radiometer channels.

The experimental results support the observation that for starting position of the mirror located at the plasma edge (corresponding to $\theta = 20^o$), despite the loss of spatial detection, the PI control can move the mirror to reach the target position and recover any loss of detection. Conversely, for starting position at the plasma center ($\theta = 30^o$) the NTM tracking is more precise, but the controller is not

able to recover stability when a loss of spatial detection occurs. This behavior depends on the DA and in large part on the limited number of radiometer channels available in the range around the ECW frequency.

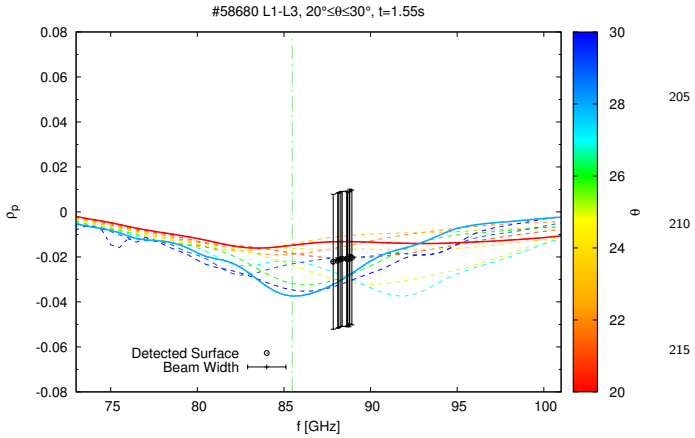

Figure 6: Difference between $L1$ and $L3$ minor radius of the emission region for Shot 58680 as function of mirrors angle and frequency

Figure 6 shows the difference between $L1$ and $L3$ minor radius of the emission region as a function of the frequency and the mirrors steering angle for Shot 58680, only for the points in the zone of successful detection. These points show that the spatial location of ECW is always smaller than the beam width. It can be noticed that using LFS ECE channels it would be possible to reach the desired frequency of $82.7GHz$ with a better accuracy.

5. Conclusions

A real time closed loop control scheme to track and suppress NTM instabilities was realized and implemented in TCV. The proof of principle of this scheme was done by mimicking quasi-in-line configuration of ECE and ECW beam.

Results show that the control algorithm was able to track the NTM instability and to aim the ECW at the NTM instability position with an accuracy smaller than the beam width. However, using only the HFS ECE channels, the control scheme was not able to follow the NTM in all possible spatial positions, in particular it was not possible to steer the mirror at the desired target position of $82.7GHz$. This is mainly due to present limitation of the radiometer and this can be partially overcome introducing new features in the detection algorithm.

Based on the successful preliminary results obtained here, a new detection scheme using all ECE channels with a more complex control, which includes an initial preprogrammed scan phase over all mirror steering angle, is being developed and will be tested in the next experimental campaign.

References

[1] M. Maraschek, Neoclassical Tearing Mode (NTM), volume 83 of *Springer Series on Atomic, Optical, and Plasma Physics*, Springer Berlin Heidelberg, 2015, pp. 259–304. URL: https://doi.org/10.1007/978-3-662-44222-7_8. doi:10.1007/978-3-662-44222-7_8.

[2] S. Coda at all., Nuclear Fusion 57 (2017) 102011. URL: http://stacks.iop.org/0029-5515/57/i=10/a=102011.

[3] M. Fontana, L. Porte, P. Marmillod, EPJ Web Conf. 147 (2017) 02005. URL: https://doi.org/10.1051/epjconf/201714702005. doi:10.1051/epjconf/201714702005.

[4] J. Berrino, E. Lazzaro, S. Cirant, G. D'Antona, F. Gandini, E. Minardi, G. Granucci, Nuclear Fusion 45 (2005) 1350. URL: http://stacks.iop.org/0029-5515/45/i=11/a=016.

[5] D. Farina, L. Figini, P. Platania, C. Sozzi, AIP Conference Proceedings 988 (2008) 128–131. URL: http://scitation.aip.org/content/aip/proceeding/aipcp/10.1063/1.2905053. doi:http://dx.doi.org/10.1063/1.2905053.

[6] L. Figini, D. Farina, D. Micheletti, N. Rispoli, C. Sozzi, Proceedings of 43rd EPS Conference on Plasma Physics (2016) 945–948.

Acknowledgment

This work has been carried out within the framework of the EUROfusion Consortium and has received funding from the Euratom research and training programme 2014-2018 under grant agreement No 633053. The views and opinions expressed herein do not necessarily reflect those of the European Commission.